Validation of Aerodynamic Parameters for High-Incidence Research Models

A. Jean Ross* and Geraldine F. Edwards†
Royal Aerospace Establishment, Farnborough, Hampshire, United Kingdom
Vladislav Klein‡
George Washington University, Hampton, Virginia
and
James G. Batterson§
NASA Langley Research Center, Hampton, Virginia

Two series of free-flight tests on high-incidence research models have been conducted to investigate flight behavior near departure conditions and to obtain responses for deriving aerodynamic data. The analysis of the first series using stepwise regression has given the structure of the mathematical model and values for the lateral derivatives for angles of attack between about 20 and 30 deg, and the results have been used in the design of active control laws. These were tested in 1986, and preliminary analysis indicates that the mathematical model is validated. Flight results for a new configuration are also discussed and compared with predicted responses.

Nomenclature

a_x,a_y,a_z	= linear accelerometer readings
C_{lp}	= rolling moment due to roll rate
$C_{l\beta}$	= rolling moment due to sideslip, per rad
C_{mq}	= pitching moment due to pitch rate
C_{np}	= yawing moment due to roll rate
$C_{n\beta}$	= yawing moment due to sideslip, per rad
$C_{Y\beta}$	= side force due to sideslip, per rad
C_l,C_m,C_n	= moment coefficients
C_X,C_Y,C_Z	= force coefficients
p,q,r	= rate of roll, pitch, yaw
$T_{\frac{1}{2}}$	= time to half amplitude, s
t	= time, s
V	= airspeed, knots or m/s
α	= angle of attack
β	= angle of sideslip
ζ	= rudder deflection, +ve to port
η_C	= canard deflection, +ve Trailing edge (TE) down
η_F	= TE flap deflection, +ve TE down
η_T	= tailplane deflection, +ve TE down
θ	= pitch attitude angle
ξ_F	= differential flap, +ve starboard down
ξ_T	= differential tail, +ve starboard down
ϕ	= bank angle

Introduction

A RESEARCH program on the aerodynamic and dynamic characteristics of a combat aircraft configuration at high angles of attack was started at the Royal Aircraft Establishment (RAE) in 1979.[1] A research configuration was designed, shown in Fig. 1, with an aft-swept wing suitable for good transonic maneuvering (although the tests discussed here are all for low speed), a closely coupled canard, and an all-moving tailplane for pitch and roll control. The single fin has a rudder, and a simple fuselage shape was chosen to ease manufacture of both wind-tunnel and free-flight models; it was also decided not to represent intakes. This high-incidence research model is known as HIRM, or HIRM1. The leading geometric data are listed in Table 1, with those of HIRM2 (described later).

The program began with a very comprehensive series of static wind-tunnel tests, followed by dynamic tests on the RAE oscillatory rig, on the British Aerospace (BAe) and RAE rotary rigs, and on the RAE large-amplitude pitch rig. These results have been published,[2-5] and some results from a further static test in the RAE 5-m tunnel were reported in Ref. 6. A model is also being tested on the whirling arm at the College of Aeronautics at Cranfield to give results for steady pitching and yawing. The results from the RAE wind-tunnel tests were used to form mathematical models of the aerodynamic forces and moments, in order to design flight experiments using large-scale free-flight models.

The results of the first series of free-flight tests on HIRM1 have been discussed in two papers. The interpretation and use of the data from the wind-tunnel experiments to obtain satisfactory simulation of flight responses are described in Ref. 6, and the results for values of the aerodynamic derivatives obtained by stepwise regression analysis of the flight data are reported in Ref. 7. This analysis established the variation of the lateral derivatives with angle of attack between 20 and 30 deg for the large-amplitude coupled oscillatory responses obtained in flight, and indicated significant effects due to the two different canard settings (0 and −10 deg) tested. A

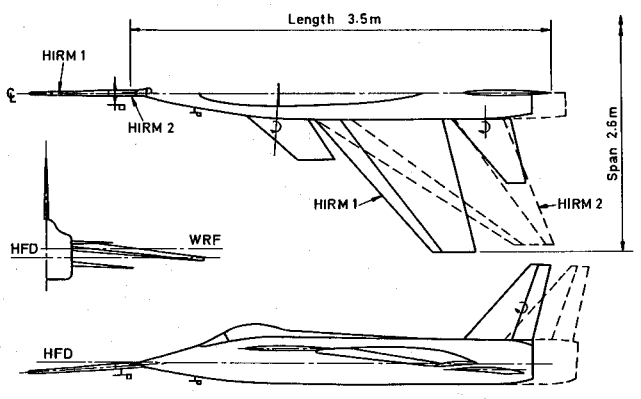

Fig. 1 High-incidence research models, HIRM1 (original) and HIRM2 (modified).

Received March 7, 1988; revision received Dec. 5, 1988.

*Head, Aircraft Dynamics Section, Aerodynamics Department. Associate Fellow AIAA.
†Senior Scientific Officer, Aircraft Dynamics Section, Aerodynamics Department. Associate Fellow AIAA.
‡Research Professor, Associate Fellow AIAA.
§Aerospace Technologist. Member AIAA.

Table 1 Leading particulars of models

	HIRM1	HIRM2
Wing (gross)		
Leading edge sweep, deg	42	58
Aspect ratio	3.3	2.3
Taper ratio	0.302	0.183
Span, m	2.6	2.5
Mean chord, m	0.868	1.259
Canard (net)		
Leading edge sweep, deg	50	50
Aspect ratio	0.86	0.86
Area ratio	0.13	0.10
Tail (net)		
Leading edge sweep, deg	42	—
Aspect ratio	1.65	—
Area ratio	0.16	—
Fin (net)		
Leading edge sweep, deg	42	42
Aspect ratio	1.66	1.66
Area ratio	0.11	0.09
Fuselage (without probe)		
Length, m	3.32	3.62
c.g. aft of nose	1.91	2.16

selection of the results is included in this paper, because the mathematical model of the lateral stability and control derivatives have been updated with these values from flight tests.

The second phase of flight tests was undertaken by the RAE trials team in 1986 at NASA Ames-Dryden. Active control systems had been designed for these flight tests by British Aerospace (Brough). One set of control laws (HIRM Aerodynamic Parameter Identification, HAPI) was designed to maintain steady longitudinal flight during lateral responses to roll and yaw control inputs, and to restore wings level if bank angle became excessive, using a switch type of control law. An alternative set of control laws (Departure Prevention System, DEPS) was designed to prevent departure from controlled flight by limiting angle of attack, and both sets of laws were implemented digitally, using the asynchronous multiprocessor system developed by Lucas Aerospace.[8]

Results from two of these flight experiments are discussed in this paper, and the other flight tests are described briefly. The responses calculated using the mathematical model based on the results in Ref. 7 are compared with flight responses, and the efficiency of the departure prevention system is demonstrated. Analysis of the records is in progress, using stepwise regression methods to give values for the aerodynamic derivatives obtained from different types of responses, particularly from small-amplitude uncoupled oscillations.

A second HIRM configuration, known as HIRM2, has also been tested in both wind-tunnel and flight experiments. The wing and tailplane of HIRM1 are replaced by a more highly-swept wing with trailing-edge flap controls, on a slightly longer fuselage, with the same canard and fin/rudder. The center of gravity for these flights was chosen to give near-neutral stability at $\alpha \simeq 25$ deg, but the pitch-up encountered on this type of configuration means that the model has to be flown with an active control system to insure satisfactory release from the towing helicopter. Control laws were designed analogous to those used for HIRM1, using results from static and dynamic wind-tunnel tests, to give controlled longitudinal responses and either controlled or unaugmented lateral responses. Some results are discussed to show that a mathematical model based on results from wind-tunnel tests (using the data in a manner analogous to that derived from experience in interpreting HIRM1 data) gives the main characteristics of the flight responses.

Free-Flight Experiments

Experiments in 1983

The first series of free-flight trials at NASA Ames-Dryden Flight Research Facility were aimed at establishing the mathematical model of the aerodynamic forces and moments obtained from responses of HIRM1 (shown in Fig. 1) without an active control system. The experiments had been designed using values of aerodynamic derivatives obtained from wind-tunnel tests, most of the data being reported in Refs. 2 and 3, and the important derivatives being given in Ref. 6.

The canard setting was held constant for each flight, at either 0 or -10 deg, and the tailplane setting was changed at intervals to give a range of trimmed angles of attack. At each tailplane setting, lateral control inputs were applied sequentially, differential tailplane doublet first, followed by rudder pulse, and finally differential canard doublet. The longitudinal responses were predicted to be of small amplitude for the changes of trim chosen, but could be affected by cross coupling, particularly after the rudder pulse. The lateral Dutch roll mode was predicted to be a divergent oscillation at some angles of attack, depending on canard setting, but simulations of the responses were acceptable.

Two factors contributed to the high cross-coupling of the actual flight responses, with large-amplitude oscillations occurring in both longitudinal and lateral motion. The first was that the trim conditions obtained from static wind-tunnel data gave lower angles of attack than experienced in flight; the second was that the Dutch roll damping predicted using oscillatory rig results is higher than indicated by the flight records. Both factors contribute to make the Dutch roll oscillation more unstable for given tailplane/canard settings, so that large-amplitude, lateral responses cause oscillations of considerable magnitude in angle of attack, giving a cumulative effect on the coupling. The changes in trim conditions were evaluated, and then combined with the data from the rotary rig, to give the better agreement between flight and simulated responses reported in Ref. 6.

Flight Experiments in 1986

Some short flights were made in the United Kingdom during the summers of 1984–1986 in preparation for the second series of trials at NASA Ames-Dryden. Various types of experiments were achieved in these latter trials, as described here:

1) Responses without the active control system, using changes in canard or tailplane settings to give pitch disturbances that cause coupled, large-amplitude oscillations, at canard settings of 0, -3, and -5 deg (two flights).

2) Small-amplitude responses with the HAPI control laws active to maintain near-constant angle of attack, with canard setting of either 0 or -5 deg; the lateral responses due to differential tail doublet or rudder pulses are unaugmented unless bank angle exceeds ± 30 deg (three successful flights, including one with c.g. at rear position, and two flights possibly yielding data).

3) Responses to combined control inputs to test the departure prevention system, at canard setting of either 0 or -10 deg (two successful flights and one possibly yielding data).

4) Responses of the new model HIRM2 (also shown in Fig. 1) with HAPI control laws active to prevent loss of control after release, and to maintain near-constant angle of attack during lateral oscillations due to differential flap and rudder inputs (two flights, but the second went into a spin).

The average length of flight is about 120 s, with 10–12 "maneuvers" performed in most flights.

Analysis of 1983 Results

The first step in the data analysis included a check on data compatibility and the estimation of unknown bias errors in the measurements. Then, from the postulated possible expres-

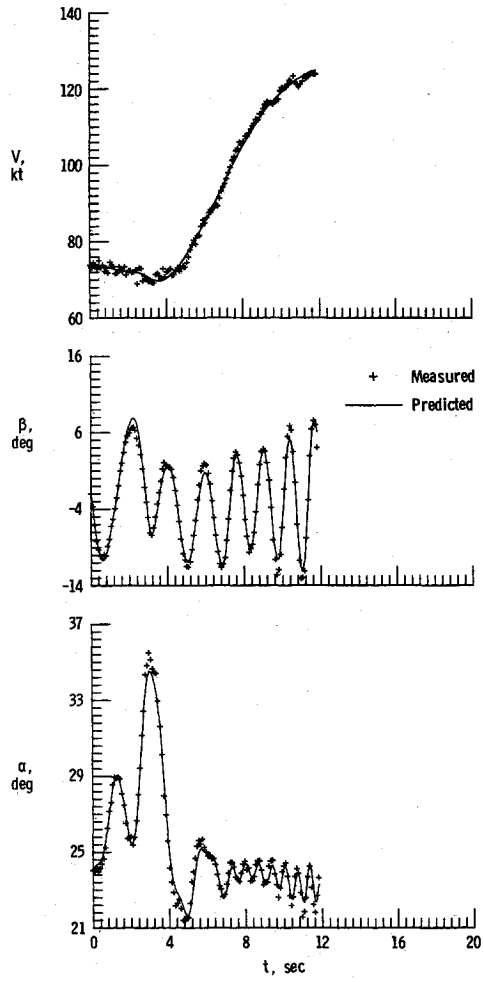

Fig. 2 Compatibility check on flight data.

Table 2 Estimates of bias errors in measured data

Measured variable	Bias	Standard error
V, m/s	1.6	0.63
β, deg	−3.4	0.25
α, deg	−1.2	0.42
ϕ, deg	−6.0	1.1
θ, deg	−1.6	0.96
a_x, g units	0.04	0.020
a_y, g units	0.06	0.031
a_z, g units	−0.12	0.015
p, deg/s	−4.0	1.8
q, deg/s	1.5	0.23
r, deg/s	−3.0	0.41

sions for aerodynamic coefficients, the algebraic structure of these coefficients was determined and unknown parameters estimated. The resulting aerodynamic model equations were verified by 1) comparison of results from individual maneuvers and partitioned data, 2) comparison of results from flight data with those from wind-tunnel measurements, and 3) checking the mathematical model prediction capabilities.

For the compatibility check, a nonlinear fixed-interval smoother was applied.[9] An example of measured and reconstructed (estimated) airspeed and angle of attack and sideslip is given in Fig. 2. In this maneuver, only constant bias and initial conditions were estimated. Because of the very good agreement between the measurements and prediction, it was not necessary to estimate the scale factors. The estimated bias errors in measured data and their standard errors are summarized in Table 2.

For the estimation of aerodynamic characteristics of HIRM1, the data from five flights with 26 maneuvers were available. One example of a test run is given in Fig. 3. It represents the motion of the model with $\eta_C = -10$ deg following its release and then the response to a differential tail doublet of duration approximately 3 s at $t = 24$ s. Two flights with $\eta_C = -10$ deg, $\eta_T \simeq -18$ deg are designated as HD1 and HD3, and the remaining three flights with $\eta_C = 0$ deg, $\eta_T \simeq -15$ deg as HD2, HD4, HD6. In addition to analyzing each of the 26 individual maneuvers, the data from all of the flights were joined together into two sets of data, one for each canard setting. The resulting ensembles were then partitioned into subsets according to the value of angle of attack (see Ref. 10 for the explanation of the partitioning procedure and its impact on model simplification). For these new subsets of data, the aerodynamic coefficients were modeled mostly on 1 deg subspaces of the original α space.

All of the corrected data from available maneuvers were analyzed by using a stepwise regression. As a modified version of the linear regression, this method can determine the structure of aerodynamic model equations and give estimates of the model parameters. The determination of an adequate model for the aerodynamic coefficients starts with the postulation of the terms that might enter the model. For individual maneuvers, the aerodynamic coefficients were postulated as functions of response and control variables and their combinations were: 1) the longitudinal coefficients C_X, C_Z, and C_m as functions of α, q, η_T, η_c, α^2, $q\alpha$, α^3, $q\alpha^2$, β^2, $\beta^2\alpha$, p, r, ξ_T, ξ_C, and ζ; and 2) the lateral coefficients C_Y, C_l, and C_n as functions of β, p, r, ξ_T, ξ_C, ζ, $\beta\alpha$, $p\alpha$, $r\alpha$, βa^2, $p\alpha^2$, $r\alpha^2$, β^2, p^2, β^3, p^3, $\beta^2\alpha$, $p^2\alpha$, $\beta^3\alpha$, $p^3\alpha$, $p\beta$, α, α^2, and α^3.

In both cases, the functions were approximated by polynomials. The variables in these polynomials represent the increments with respect to their trim values. In the equation for pitching-moment coefficient, the term $\dot{\alpha}$ could not be explicitly included because of identifiability problems that occur due to high correlation between $\dot{\alpha}$ and q.

Relationships between parameters in the expression for C_m with and without the explicit $\dot{\alpha}$ terms can be found in Ref. 11. For the partitioned data, the polynomials representing aerodynamic coefficients were postulated without explicit α-dependent terms, since the partitioned subspaces span only 1 deg range.

The general form of the aerodynamic model equations can be written as

$$y(t) = \theta_0 + \theta_1 x_1(t) + \cdots + \theta_n x_n(t) \tag{1}$$

where $y(t)$ represents the resultant coefficient of the aerodynamic force and moment, $\theta_1, \ldots, \theta_n$ are the stability and control derivatives, θ_0 is the value of any particular coefficient corresponding to the initial conditions, and $x_1, \ldots, x_n$ are the HIRM response and control variables or their combinations. The stepwise regression is a model-building algorithm using the least-squares method. All significant terms among the candidate variables are determined and the corresponding parameters are estimated. The variable chosen for entry into the regression equation is the one that has the largest correlation with y after adjusting for the effect on y of the variables already selected. The parameters are estimated by minimizing the cost function

$$J = \sum_{i=1}^{N} \left[y(i) - \theta_0 - \sum_{j=1}^{l} \theta_j x_j(i) \right]^2 \tag{2}$$

where $l + 1$ is the number of parameters in the regression equation.

At every step of the regression, the variables incorporated into the model in the previous steps and a new variable entering the model are re-examined. Any variable that produces a statistically insignificant contribution is removed from the model. The process of selecting and checking variables continues until no more variables are admitted into or rejected from the equation. The details of the whole procedure are explained in Refs. 11 and 12.

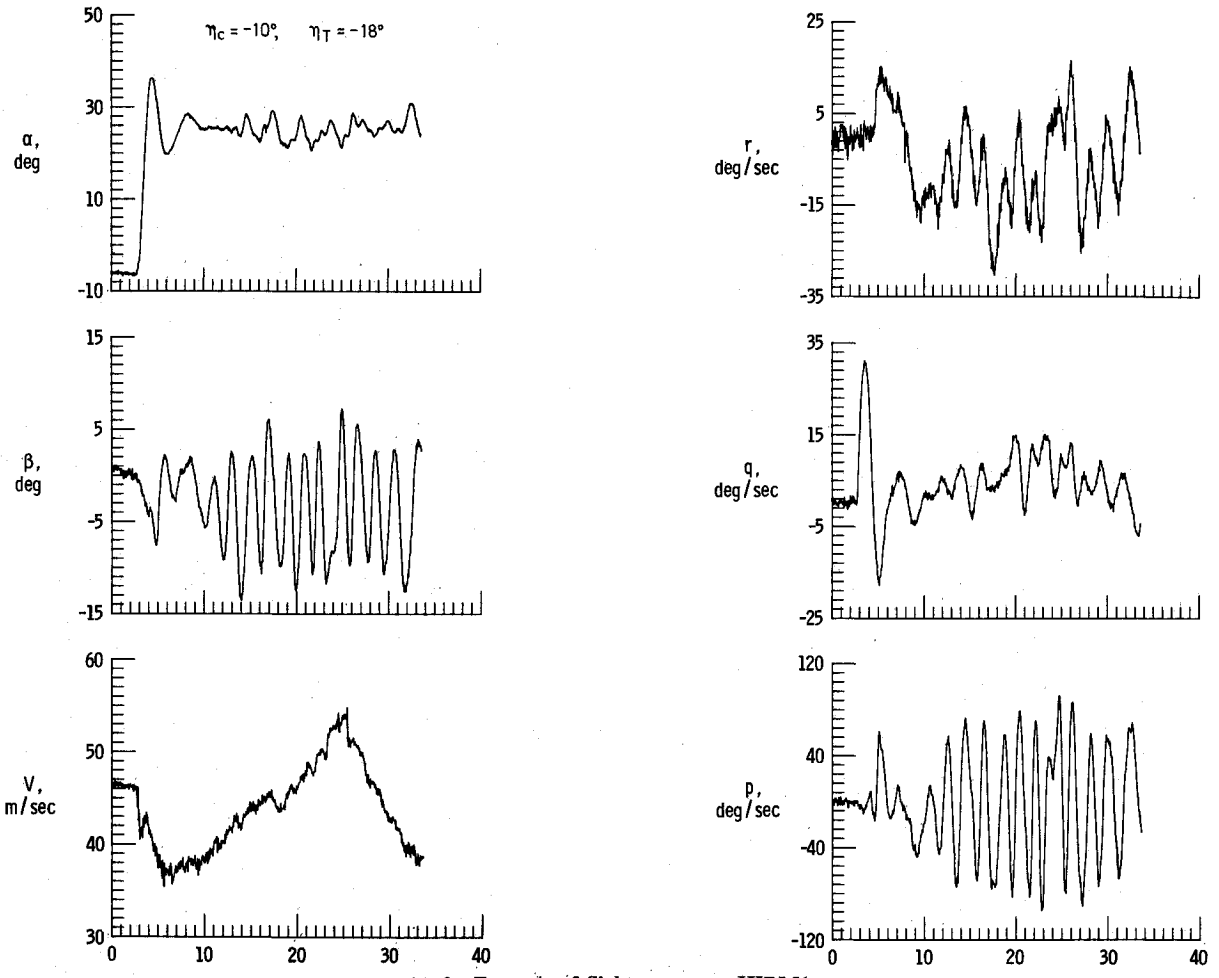

Fig. 3 Example of flight responses, HIRM1.

The type of HIRM1's responses, and the design of the flight experiments, means that the main emphasis in the data analysis was constrained to the lateral aerodynamic equations. Some of the important lateral parameters are presented to show their variation with angle of attack and canard setting, and their agreement with wind-tunnel test results. Three maneuvers in flight HD1 and one in the HD3 consisted mostly of lightly damped large-amplitude oscillations (see, for example, Fig. 3). The remaining three maneuvers in HD3 flight exhibited large excursions in α with some lateral coupling. The stepwise regression procedure demonstrated that for the oscillatory maneuvers analyzed as partitioned data, models with linear parameters were adequate for all three lateral coefficients C_Y, C_l, and C_n. From the analysis of the individual maneuvers, the technique also selected nonlinear terms $\beta\alpha$ and $p\alpha$ for the model equations for the coefficient C_n. The aerodynamic derivatives $C_{Y\beta}$, $C_{l\beta}$, and $C_{n\beta}$ were always selected by the technique as the first parameters for the model equations. They also explain the substantial part of the variations in measured data. High sensitivity of the experimental data to these derivatives sometimes resulted in identifiability problems for the remaining parameters, e.g., lower accuracy of their estimates.

The estimated values of three static parameters $C_{Y\beta}$, $C_{l\beta}$, and $C_{n\beta}$ from data of flights HD1 and HD3 are presented in Fig. 4. The parameter values of $C_{Y\beta}$ from flight HD3 are not available because of a malfunction of the lateral accelerometer. From the plot of $C_{Y\beta}$ against α, it is evident that the flight data are consistent, but for $\alpha \leq 23$ deg the flight data are lower than those from the wind-tunnel static and oscillatory measurements. The estimates of $C_{l\beta}$ from each flight show certain inconsistency for $\alpha < 25$ deg, but on the average they

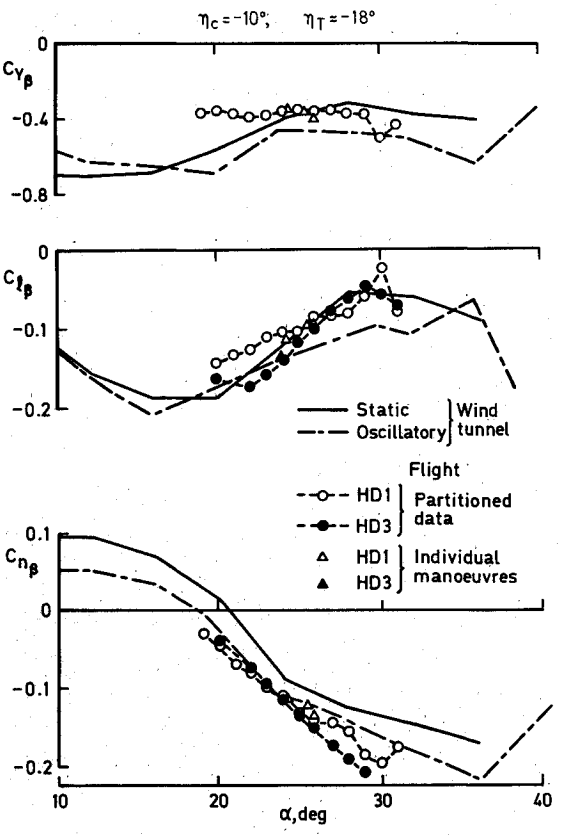

Fig. 4 Derivatives due to sideslip, HIRM1 with canard −10 deg.

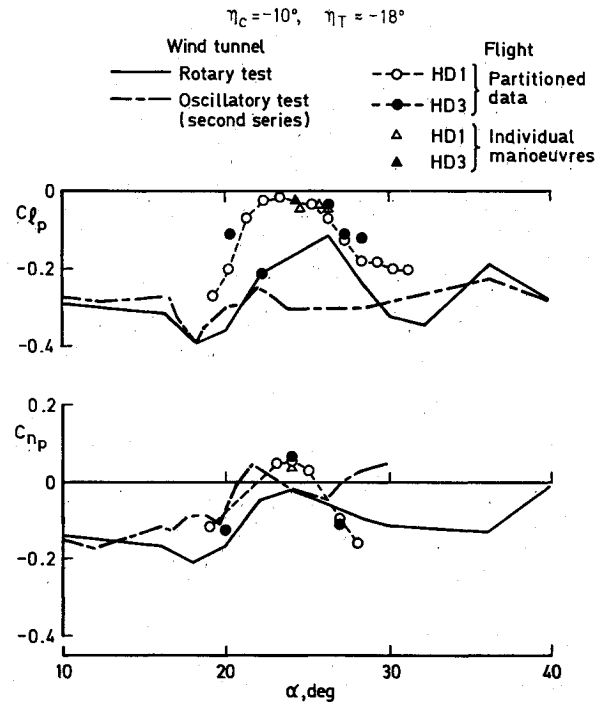

Fig. 5 Derivatives due to roll rate, HIRM1 with canard −10 deg.

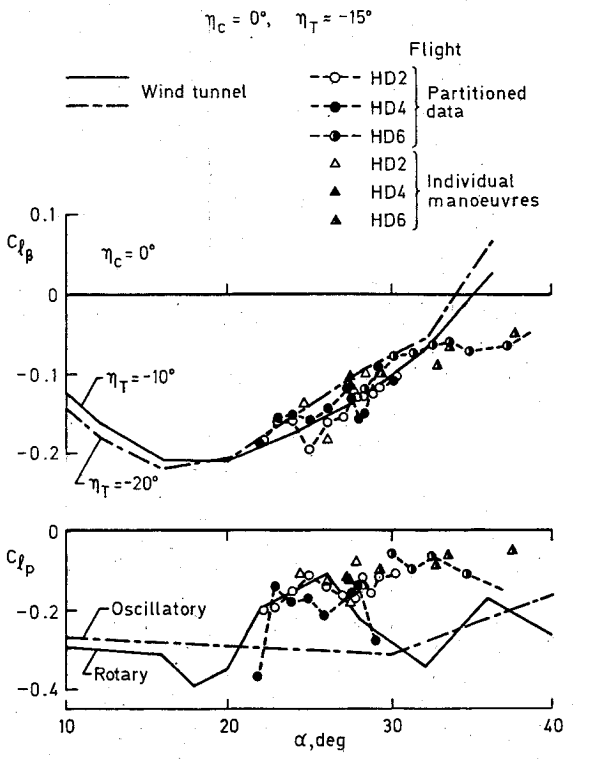

Fig. 6 Rolling moment derivatives, HIRM1 with canard 0 deg.

agree well with the wind-tunnel static data. Finally, the flight estimates of $C_{n\beta}$ are consistent between flights and agree with the wind-tunnel oscillatory data, but show more directional instability of HIRM1 than predicted by the wind-tunnel static measurements.

In Fig. 5, the damping derviative C_{lp} and cross derivative C_{np} are compared with the results from the oscillatory and rotary wind-tunnel tests. The rotary data predicted a decrease in damping for 20 deg $< \alpha <$ 28 deg; whereas, the oscillatory tests show no deterioration in this region. [It should be noted that oscillatory rig tests give the combined derivatives (e.g., $C_{lp} + C_{l\beta} \sin\alpha$), so differences can be expected at high angles

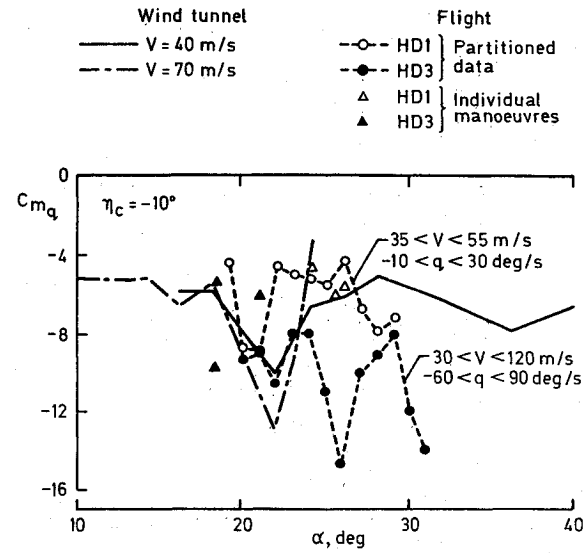

Fig. 7 Damping in pitch derivative, HIRM1 with canard −10 deg.

of attack.] Results from the second series of oscillatory tests indicate some sensitivity to angle of attack near 20 deg, but no severe loss in damping was experienced as angle of attack was being changed between test points. The flight data indicate even less damping-in-roll than the rotary test. The flight results are in agreement with the observed responses of the drop model, which show very little damping or no damping at all. The reason for the discrepancy between the oscillatory data and flight results can be due to the different amplitude of oscillations in the wind tunnel ($\pm$2 deg) and in flight (around $\pm$35 deg), the reduced frequencies being about 0.03 in both cases. The comparison of C_{np} parameters from various tests shows satisfactory agreement, particularly if it is noted that all values are near zero in this angle-of-attack range.

The effect of different canard settings is shown in two examples where $\eta_C = 0$ deg and $\eta_T = -15$ deg. In the upper part of Fig. 6, the parameter estimates of $C_{l\beta}$ from flights HD2, HD4 and HD6 are plotted and compared with wind-tunnel data for $\eta_T = -20$ and -10 deg. The consistency of flight estimates is good, and they agree with the wind-tunnel data for $\alpha < 32$ deg. For higher α, the flight results still exhibit negative values for $C_{l\beta}$, but the wind-tunnel measurements predict zero and positive dihedral effect. To confirm these differences, more flight data would be needed for $\alpha > 32$ deg. The lower part of Fig. 6 contains the damping parameters C_{lp} from flight and wind-tunnel testing. The rotary test results agree with flight data for 22 deg $< \alpha <$ 27 deg. For the α region between 27–35 deg, the flight data still indicate low damping-in-roll, which is not confirmed by wind-tunnel measurements. A comparison of flight results in Figs. 5 and 6 indicates strong effect of canard setting on damping-in-roll, not seen in the wind-tunnel data.

Some of the single maneuvers and partitioned data sets were also analyzed in order to obtain the estimates of longitudinal aerodynamic parameters. The results for the coefficients of the longitudinal and vertical forces were very limited and inconsistent due to insufficient excitation of the airspeed and heave motion. More consistent results were obtained, however, for the pitching-moment parameters. Both the individual maneuvers and partitioned data provided good estimates for the damping and control derivatives and also indicate effects of yawing and rolling velocities on C_m. Figure 7 presents the estimates of C_{mq} derivative from flights HD1 and HD3. The discrepancy in these results could be caused by different flight conditions and the amplitudes of pitching velocity. The low-amplitude results agree well with wind-tunnel measurements. The second set of flight results shows an increased damping in pitch.

Results from 1986 Trials

The initial analysis of two flights are discussed, by comparing flight responses with simulations, to give a measure of the adequacy and accuracy of the mathematical models used for the aerodynamic forces and moments. The validation of the HIRM1 model is also demonstrated by the efficiency of the departure prevention system, and the results of one such flight test are described. The detailed analysis of the flight records is in progress, using stepwise regression and possibly maximum-likelihood techniques.

Coupled Oscillations of HIRM1

An experiment was planned specifically to validate the mathematical model based on the results obtained from regression analysis of the coupled oscillations described in the previous section. The values of the derivatives shown in Figs. 4–6 were used in the simulation, with wind-tunnel data providing the longitudinal forces and moments. Linear interpolation was used to obtain values of the derivatives for canard settings of −3 and −5 deg from the values for 0 and −10 deg. The control inputs were step changes in either canard or tailplane setting to give a change in trimmed angle of attack, but the asymmetric forces and moments present at these flight conditions cause lateral responses. The Dutch roll oscillation is either lightly damped or divergent in the range of angle of attack being investigated, so the resulting coupled oscillations can be of large amplitude.

The results from the previous flights indicate that HIRM1 is near-neutrally stable longitudinally for 21 deg $< \alpha <$ 26 deg, so the trimmed angle of attack varies significantly with canard/tailplane setting. The damping of the Dutch roll oscillation is highly dependent on angle of attack in this region, as shown in Fig. 8. It is found that the simulations give the basic characteristics of the responses, but detailed comparisons are not easily obtained because of the coupling between longitudinal and lateral motions. The characteristics of the responses for a sequence of five changes to tailplane setting are summarized in Table 3.

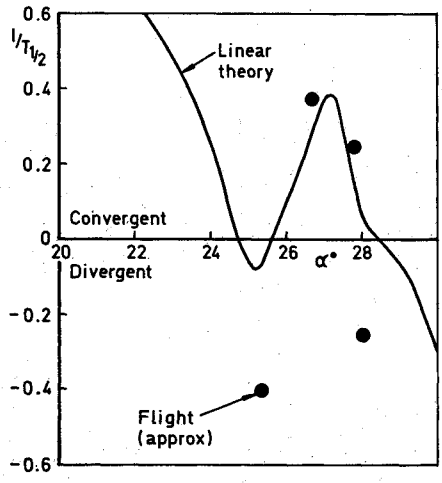

Fig. 8 Damping of lateral oscillation, HIRM1 with canard 0 deg.

In flight, the first divergent lateral oscillation is of limited amplitude, and this damps out when the angle of attack increases after the tailplane change at 22 s. The lightly damped and slowly divergent oscillations, which follow as angle of attack is increased, again are of relatively small amplitude, up to ±20 deg/s, so the coupling is not significant. Simulations starting with the flight values for all of the variables give a similar divergent oscillation of slightly larger amplitude for the first sequence, but the coupling causes larger changes in angle of attack, so that the change in tailplane setting leads to a different trim state being established, with higher values of mean angle of attack and a limit cycle in roll rate. This affects the conditions when the tailplane setting changes subsequently, so correlation between flight and simulation is lost. However, the observed convergence and divergence rates of the lateral oscillations are near those obtained from the Dutch roll mode of the linearized mathematical model, as shown in Fig. 8. The influence of the coupling on the trim states and on the formation of limit cycles is being investigated.

Such effects of coupling are illustrated in Fig. 9, where the sequence previously described is followed by a change in canard setting. This causes a divergent oscillation laterally, which appears to limit at about ±50 deg/s in roll rate. The simulation with initial conditions taken from flight records, i.e., $p = 5.6$ deg/s, $r = -3$ deg/s, $\phi = -11.6$ deg, $\beta = 0$ deg for the lateral variables, leads to a limit cycle of ±80 deg/s in roll rate after a sudden increase in angle of attack not seen in the flight records. If the simulation is started with zero values for lateral variables, the lateral oscillations are of small amplitude, slowly diverging as shown in Fig. 9. With nonzero value for either roll rate or yaw rate, the limit cycle develops to the same amplitude of ±80 deg/s.

It will be interesting to see whether the values of the lateral derivatives obtained from these flight records show a dependence on amplitude of oscillation, causing the differences between flight and simulation, or whether the sensitivity to angle of attack precludes absolute correlation of long sequences of responses when the motion is highly coupled.

HIRM2 with HAPI Control System

The mathematical model of the aerodynamic forces and moments of HIRM2 is based solely on results from wind-tunnel tests on an exact 4/9 scale model. The static tests have not been so extensive as those conducted on HIRM1,[2] and some extrapolations for control powers and effects of flap settings have had to be made. The normal force, axial force, and pitching moment are represented in data tables as functions of

Table 3 Characteristics of responses to sequence of tailplane settings

Time, s	11–22	22–29	29–42	42–55	55–63
Canard	0	0	0	0	0
Tailplane	−14.2	−13.75	−14.15	−14.55	−15.1
Flight					
Mean α deg	25.5	26.7	27.7	28.0	28.5
Lateral roll rate	Divergence to ±60 deg/s	Convergence	Lightly damped	Slow divergence	Convergence
$T_{\frac{1}{2}}$, s	−2.5	2.7	4	−4	?
Theory					
Trim α deg	25.4	21.9	24.8	26.7	28.2
$T_{\frac{1}{2}}$ at flight −α, s	−20	3	6	17	−50
Simulation					
Mean α deg	24	>30	20	>30	21

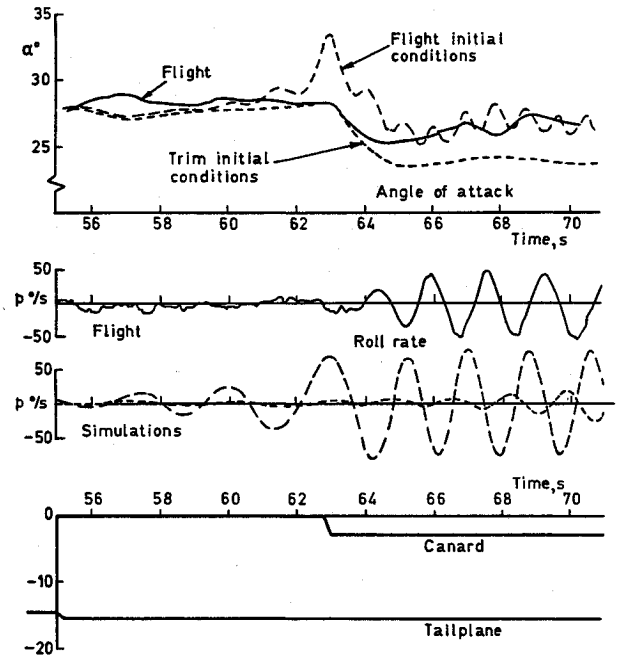

Fig. 9 Flight and simulated responses of coupled oscillations HIRM1 without active control system.

angle of attack and flap setting, with increments added for changes due to canard setting. Sideslip data depend significantly on angle of attack, and the sideforce, rolling and yawing moments measured at zero sideslip are used to account for the effect of the asymmetric nose vortices. The dynamic data were obtained from large-amplitude pitch tests for damping-in-pitch, from rotary rig tests for derivatives due to roll rate, and from oscillatory rig tests for derivatives due to yaw rate.

There have been engineering difficulties in producing acceptable responses from the actuators and drivers for the flaps, and the flights were achieved using only the inboard flaps for both roll and pitch controls. The mathematical model of the actuation system continues to be under investigation, and an approximation has been used in the simulations based on the results for the HIRM1 actuators, with an added representation of the apparent sticking observed in the flight records of HIRM2. Thus, the simulated response of the flaps cannot be expected to agree in detail with the noisy flight responses, although the general character appears to be similar.

An example of the type of responses obtained using the HAPI control system is shown in Fig. 10. After release, the flaps move quickly toward positive deflections in order to control pitch rate, and so angle of attack, and then revert to negative deflections for the requested trim condition of $\alpha = 24$ deg. The flaps are also deflected differentially, to overcome the lateral disturbance experienced at release, the bank-angle-hold control law being in operation for 5 s after release (Fig. 10a), by which time the model is flying steadily. The responses in the motion variables are not very oscillatory, and the test of the accuracy of the aerodynamic mathematical model (which the active control system is having to overcome) is the comparison of the time histories of the control movements. The symmetric flap deflection (pitch control) agrees reasonably well with this rapid maneuver after release, both in amplitude and timing, as shown in Fig. 10a. The differential flap and rudder deflections indicated in the simulation are larger in amplitude than the measured values. This is probably due to the variation of the moments due to asymmetric vortices with angle of attack assumed in the simulation, which determines the amplitude of the bank angle.

The model flew steadily until about 19 s, but bank angle was increasing negatively due to some form of asymmetry.

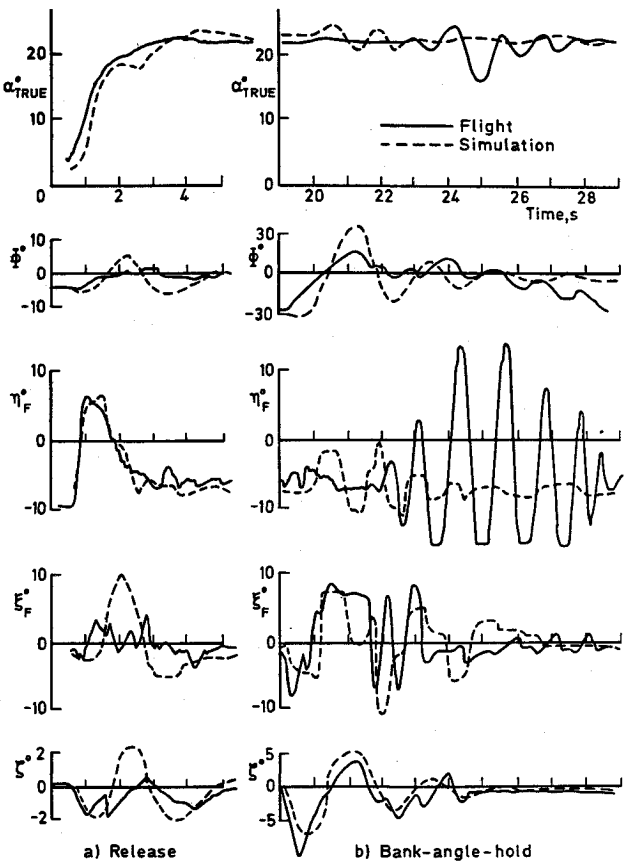

Fig. 10 Flight and simulated responses for HIRM2 with HAPI control system.

Comparable bank angles can be obtained from simulation, using asymmetric force and moments measured on HIRM2 in static wind-tunnel tests at zero sideslip. When the bank angle reached -30 deg, the lateral control law was automatically switched on (Fig. 10b), suppressing the demand to roll control programmed to occur at 20 s. The flap movements are larger than predicted, so the limit of control travel (-15.6 deg) is reached several times, causing instability, but the oscillation stops when the control law switches off. The differential flap movement is initially similar to that predicted, and the simulated response of the rudder agrees quite well with the flight records. In flight, the bank angle decreases again to -30 deg at 29 s, and the responses in differential flap and rudder due to the control law are closer to those expected, without limiting. The model flew for 130 s before being recovered, giving flight records of changes in trim state and lateral responses due to demanded rudder pulse, differential flap doublets, and to ϕ-hold control law.

Efficiency of DEPS for HIRM1

The last part of a flight of HIRM1, with canard set at -10 deg, is shown in Fig. 11, where the demands are 1) a rolling pull from $\alpha = 25$ to 27 deg initiated at about 93 s after release, 2) a coordinated turn using roll and yaw controls at 103 s, and 3) cross roll and yaw controls to induce departure at 113 s. The earlier part of the flight was designed to test the control system with roll control demands at $\alpha = 25$ and 27 deg, and the responses were as expected. The simulated responses to the combined control inputs are also in agreement with the flight results, but they are not included in Fig. 11.

Without the active control system, the responses at these angles of attack are very oscillatory in both longitudinal and lateral motions due to the coupling via the large amplitudes in roll rate, as shown in Fig. 3, particularly at this canard setting. The combined control demands tested here would

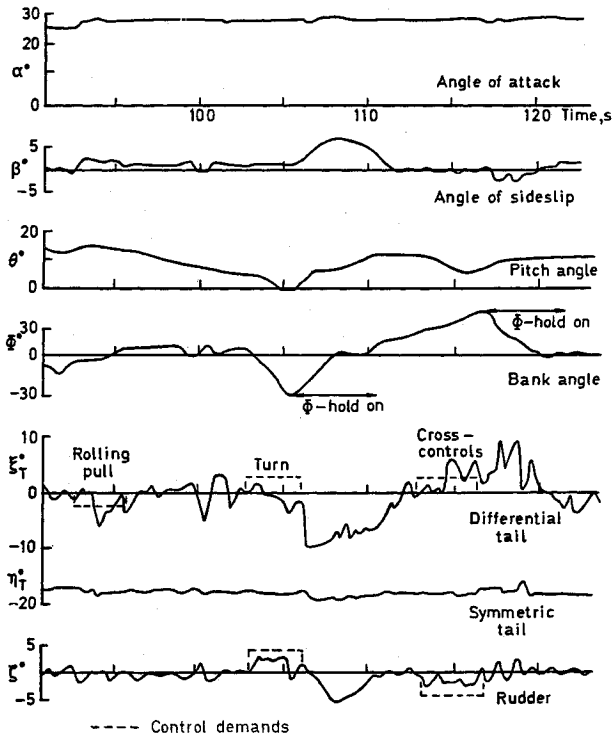

Fig. 11 Combined control inputs at high angle of attack for HIRM1 with DEPS control system.

induce departure to higher angles of attack, so the lateral control laws have to be powerful, using feedbacks in roll and yaw rate, and angles of attack, sideslip, and bank. The values of the gains depend fairly strongly on the mathematical model used in the design of the control laws, so the fact that the responses show no sign of departure indicates that values of derivatives are reasonable. The bank-angle limit was kept at 30 deg, giving only low turn-rate capability, but it may be possible to try further experiments with higher limits in flight trials in the United Kingdom.

The demanded changes to angle of attack and roll rate used to make the rolling pull cause an acceptably smooth change in flight condition at 93 s, and the mean deflection of the tailplane changes to the new trim value, whereas the differential tail deflections needed to stabilize the lateral response are of fairly large amplitude. A small lateral disturbance at 99 s (perhaps caused by asymmetries) activates the lateral control laws again, but the motion is fairly steady when the demands for the coordinated turn occur. The angle of attack remains steady until the bank angle reaches −30 deg, when the ϕ-hold law is switched on. This causes coordination to be lost, the angle of sideslip increasing to about 10 deg before returning to zero, but the angle of attack remains near the demanded value. The simulated responses show similar characteristics (not shown), but a small-amplitude oscillation is apparent on most of the variables. A small residual roll rate of about 5 deg/s occurs both in flight and in the simulation, so the ϕ-hold switches on when $\phi = +30$ deg is reached at the end of the cross-control demand input. The model recovers to steady flight with minimum of change to angle of attack, although the tailplane surfaces and rudder have to respond rapidly to maintain stability.

The flight test conducted with canard set at 0 deg had the same demands described above, and the responses are very similar. It is interesting to note that the bank angle remained below 30 deg after the cross-control demand, so that the ϕ-hold law was not operative. The angle of attack and sideslip remained near constant throughout the maneuver, giving added confidence in both the design of the control laws and the values used in the mathematical model.

Concluding Remarks

The analysis of the 1983 flight tests of HIRM1 using regression techniques has given values of aerodynamic forces and moments that compare with results from wind-tunnel experiments, although there are some significant differences. The preliminary comparison of predicted responses with the observed data from the 1986 flight tests indicates that the mathematical model based on these results is satisfactory, although it has not been possible as yet to reproduce exact correlation due to the high degree of coupling and to the sensitivity of lateral damping to angle of attack. The adequacy of the mathematical model has also been demonstrated by the flight behavior obtained with the active control system DEPS, designed to prevent departure at angles of attack up to about 30 deg.

The experience gained in interpreting the data from wind-tunnel tests on HIRM1 has been used to form the first mathematical model for the HIRM2 configuration. It is necessary to use an active control system to limit angle of attack, and the responses obtained in flight have similar characteristics to those predicted.

The detailed analysis of the flight records is continuing, and should yield aerodynamic data from small-amplitude responses for both HIRM1 and HIRM2, and from large-amplitude responses for HIRM1, for comparison with existing results.

Acknowledgments

The research work at College of Aeronautics, Cranfield, is being conducted under a UK Ministry of Defence (Procurement Executive) [MOD(PE)] Research Agreement, and that at BAe (Brough) under MOD(PE) Research Contract. The flight tests conducted by RAE at NASA Ames-Dryden, and the analysis of flight data undertaken by NASA Langley, are activities under the NASA/MOD(PE) Collaborative Agreement.

References

[1]Moss, G. F., Ross, A. J., and Butler, G. F., "A Programme of Work on the Flight Dynamics of Departure Using a High-Incidence Research Model (HIRM)," Royal Aircraft Establishment, Farnsborough, 1982 (unpublished).

[2]Ross, A. J. and Reid, G. E. A., "The Development of Mathematical Models for a High-Incidence Research Model (HIRM). Part 1: Analysis of Static Aerodynamic Data," Royal Aircraft Establishment, TR83037, 1983.

[3]Ross, A. J. and Reid, G. E. A., "The Development of Mathematical Models for a High-Incidence Research Model (HIRM). Part 2: Analysis of Dynamic Aerodynamic Data," Royal Aircraft Establishment, TR84072, 1984.

[4]O'Leary, C. O., "Dynamic Tests on a High-Incidence Research Model (HIRM) in a Low-Speed Wind Tunnel, Royal Aircraft Establishment, TR84111, 1984.

[5]O'Leary, C. O. and Rowthorn, E. N., "New Rotary Rig at RAE and Experiments on HIRM," *AGARD Conference Proceedings* 386, Paper 19, 1985.

[6]Ross, A. J. and Edwards, G. F., "Correlation of Predicted and Free-Flight Responses Near Departure Conditions of a High-Incidence Research Model," *AGARD Conference Proceedings* 386, Paper 31, 1985.

[7]Klein, V. and Mayo, M. H., "Estimation of Aerodynamic Parameters from Flight Data of a High-Incidence Research Model," ICAS 86-5.5.2, Sept. 1986.

[8]Naseem, M. and Bradley, J., "High-Incidence Research Models, Flight Control System Design," British Aerospace Rept. YAC 386, 1987.

[9]Bach, R. E. r, Jr., "A Variational Technique for Smoothing Flight-Test and Accident Data," AIAA Paper 80-1601, 1980.

[10]Batterson, J. G. and Klein, V., "Partitioning of Flight Data for Aerodynamic Modeling of Aircraft at High Angles of Attack," AIAA Paper 87-2621, Aug. 1987.

[11]Klein, V., Batterson, J. G., and Murphy, P. C., "Determination of Airplane Model Structure from Flight Data Using Modified Stepwise Regression," NASA TP-1916, 1981.

[12]Klein, V. and Batterson, J. G., "Determination of Airplane Model Structure from Flight Data Using Splines and Stepwise Regression," NASA TP-2126, 1983.